Diastereoisomeric Organophosphorus Compounds. Part 4.[1-3] Proton and Phosphorus-31 Nuclear Magnetic Resonance Spectra of Compounds of the Type $[RR'P(X)]_2Y$ and $RR'P(X)-Y-(Z)PRR'$ ($R = CH_3$, $R' = t\text{-}C_4H_9$)

G. Hägele,* G. Tossing, W. Kückelhaus, and J. Seega
Institut für Anorganische Chemie und Strukturchemie der Universität Düsseldorf, D-4000 Düsseldorf, German Federal Republic
R. K. Harris *
School of Chemical Sciences, University of East Anglia, Norwich NR4 7TJ

When R and R' are simple alkyl groups, compounds of the type $[RR'P(X)]_2Y$ give rise to $[AR_tX_n]_2$ spectra (assuming X and Y are non-magnetic). Explicit expressions for resonance frequencies and intensities of A (^{31}P) and R and X (^1H) are derived. Data are given for *rac*-$[RR'P]_2$, *meso*-$[RR'P(S)]_2$, *rac*-$[RR'P(S)]_2$, *meso*-$[RR'P(S)]_2O$, and *rac*-$[RR'P(S)]_2S$. The results are discussed and compared to those for asymmetric compounds of the type $RR'P(S)-PRR'$ and $RR'P(S)-S-PRR'$.

Chiral diphosphane structures give rise to diastereoisomerism as indicated in Scheme 1. In isotropic solution two different specific n.m.r. spectra will be observed, distinguishing the *meso* [$R_{(P)}S_{(P)}$, $S_{(P)}R_{(P)}$]-form from the racemic [$R_{(P)}R_{(P)}$, $S_{(P)}S_{(P)}$] pair. Since solution-state n.m.r. *a priori* does *not* enable the assignment of diastereospecific data sets, previous work concerning $[RR'P(X)]_2Y$ was based mainly on relatively intangible considerations of analogies.[4-11] Absolute confirmation of the stereochemically important n.m.r. parameters such as δ_H, δ_P, J_{PH}, and J_{PP} can only be obtained by combining *X*-ray and n.m.r. studies.

In preceding papers[1,4] we described the synthesis and crystal and molecular structures of the compounds in Scheme 2. Our particular interests were drawn to symmetric model systems with X = Z. The compounds $[RR'P(X)]_2Y$ give rise to symmetric spin systems of the general type $[AR_tX_n]_2$. Explicit algebraic expressions for the resonance frequencies and intensities of R and X were derived[4,5] to explain[6] the ^1H n.m.r. pattern of one diastereoisomeric form of $[CH_3(t\text{-}C_4H_9)P(S)]_2$. Here we give a detailed account of spectral features of A (^{31}P), R and X (^1H) resonances for well defined model systems such as: *rac*-$[CH_3(t\text{-}C_4H_9)P]_2$ (1b), *meso*-$[CH_3(t\text{-}C_4H_9)P(S)]_2$ (2a), *rac*-$[CH_3(t\text{-}C_4H_9)P(S)]_2$ (2b), *meso*-$[CH_3(t\text{-}C_4H_9)P(S)]_2O$ (3a), and *rac*-$[CH_3(t\text{-}C_4H_9)P(S)]_2S$ (4b).

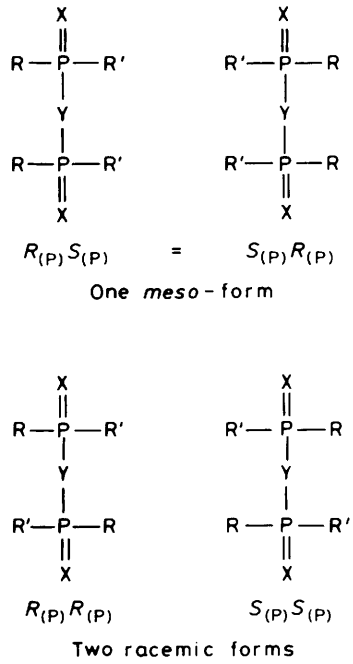

Scheme 1.

$RR'P(X)-Y-(Z)PRR'$ with $R = CH_3$ and $R' = t\text{-}C_4H_9$

No.	X	Y	Z	References to synthesis	Structures	
(1)	l.p.	—	l.p.	1,3		
(2)	S	—	S	1,3	*meso* [2]	*rac* [2]
(3)	S	O	S	3,4	*meso* [3]	
(4)	S	S	S	1		*rac* [2]
(5)	S	—	l.p.	1		
(6)	S	S	l.p.	1		

Scheme 2. l.p. = Lone pair

Theoretical

The description of the spin system in Scheme 3 will be used in our discussion of the spectral analysis of the $[AR_tX_n]_2$ spin system. There are 12 independent n.m.r. parameters which in principle affect the spectra, *viz.*: $\nu_A = \nu_{A'}$, $\nu_R = \nu_{R'}$, and $\nu_X = \nu_{X'}$; $J_{AA'}$, $J_{RR'}$, $J_{XX'}$, $J_{AX} = J_{A'X'}$, $J_{AR} = J_{A'R'}$, $J_{RX} = J_{R'X'}$, $J_{AX'} = J_{A'X}$, $J_{AR'} = J_{A'R}$, and $J_{RX'} = J_{R'X}$. Determination of the chemical shifts ν_A, ν_R, and ν_X is trivial since, under the assumption that $|\nu_R - \nu_X| \gg |J_{RX}|$ (and correspondingly for the A,X and A,R pairs of groups) the three n.m.r. bands are symmetrical about their respective chemical shifts. Moreover, in the cases considered here $J_{RR'}$, $J_{XX'}$, J_{RX}, and $J_{RX'}$ are long range in nature and are negligibly small. Consequently the appearance of each band in the spectrum can depend only on five coupling parameters. Simple algebraic solutions to the eigenvalue problem may be achieved, and these will be presented below.

The expressions for the R and X regions have been the subject of a previous note,[5] but they have now been cast in a different form, quoted below, for convenience of computing, and applied to a number of new examples. The equations for the X region have not been presented in the open literature before. The derivation of the equations proceeds along the same lines as for [12,13] the simpler $[AX_n]_2$ spin system. However,

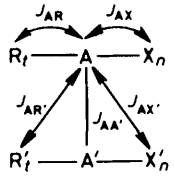

Scheme 3.

it should be noted that in the $[AR_tX_n]_2$ case the R region of the spectrum depends, *inter alia*, on J_{AX} and $J_{AX'}$, which is at first sight surprising.

It will prove useful to define linear combinations as in equations (i)—(iv). Since N_{AR} and L_{AR} are obtained independently from the spectra, it is evident that the relative signs of J_{AR} and $J_{AR'}$ are accessible (as are the relative signs of J_{AX} and $J_{AX'}$). However, the single-resonance spectra do not depend on any other relative signs of coupling constants.

$$N_{AR} = J_{AR} + J_{AR'} \quad \text{(i)}$$

$$L_{AR} = J_{AR} - J_{AR'} \quad \text{(ii)}$$

$$N_{AX} = J_{AX} + J_{AX'} \quad \text{(iii)}$$

$$L_{AX} = J_{AX} - J_{AX'} \quad \text{(iv)}$$

The Spectra of the A *Nuclei.*—The A spectra in $[AR_tX_n]_2$ systems are symmetrical with respect to ν_A. They may easily be broken down into a series of overlapping ab subspectra. Here we adopt the usual symbols describing the ab subspectrum (Scheme 4). Since the A and A' nuclei couple to the R_t, R'_t, X_n, and X'_n groups effective Larmor frequencies may be defined as in equations (v) and (vi) where m_R, $m_{R'}$, m_X, and $m_{X'}$ are the total component-spin quantum numbers of the composite particles in groups R_t, R'_t, X_n, and X'_n, respectively, and may take the following values: $-\frac{t}{2} \cdots m_R$ or $m_{R'} \cdots +\frac{t}{2}$ and $-\frac{n}{2} \cdots m_X$ or $m_{X'} \cdots +\frac{n}{2}$. $(t + 1)$ and $(n + 1)$ different states exist for m_R,$m_{R'}$ and m_X, $m_{X'}$ respectively. Therefore $(t + 1)^2(n + 1)^2$ ab-type subspectra comprise the total A part of the $[AR_tX_n]_2$ spectrum. Such ab subspectra are located at frequencies $\nu_{av.}$ [equation (vii)]. The differences, $\Delta\nu$, in effective Larmor frequencies are given by equation (viii). Of the ab-type subspectra described above, $(t + 1)(n + 1)$ will fall actually into the a_2 category, corresponding to situations with $m_R = m_{R'}$ and $m_X = m_{X'}$, leading to $\Delta\nu = 0$. Such subspectra will give rise to singlet lines located at $\nu_{av.} = \nu_A + 2m_RN_{AR} + 2m_XN_{AX}$ and having relatively strong intensities given by equation (ix). In practice a successful analysis of such a_2 singlets will give information about N_{AR} and N_{AX}. For L_{AR}, L_{AX}, and $J_{AA'}$ a total analysis of the A spectrum is required. In addition to the $(t + 1)(n + 1)$ a_2 subspectra, there are $\frac{1}{4}t(t + 1)n(n + 1)$ *different* ab subspectra.

$$\nu_a = \nu_A + m_RJ_{AR} + m_{R'}J_{AR'} + m_XJ_{AX} + m_{X'}J_{AX'} \quad \text{(v)}$$

$$\nu_b = \nu_A + m_RJ_{AR'} + m_{R'}J_{AR} + m_XJ_{AX'} + m_{X'}J_{AX} \quad \text{(vi)}$$

$$\nu_{av.} = \nu_A + (m_R + m_{R'})N_{AR} + (m_X + m_{X'})N_{AX} \quad \text{(vii)}$$

$$\Delta\nu = (m_R - m_{R'})L_{AR} + (m_X - m_{X'})L_{AX} \quad \text{(viii)}$$

$$I = 4\binom{t}{\frac{t}{2} - m_R}^2\binom{n}{\frac{n}{2} - m_X}^2 \quad \text{(ix)}$$

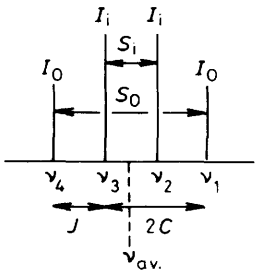

Variables	Frequencies	Intensities
$\Delta\nu = \nu_a - \nu_b$	$\nu_1 = \nu_{av.} - \frac{1}{2}S_o$	$I_1 = I_1 = I_4 = 1 - \lvert J/2C \rvert$
$\nu_{av.} = \frac{1}{2}(\nu_a + \nu_b)$	$\nu_2 = \nu_{av.} - \frac{1}{2}S_i$	$I_o = I_2 = I_3 = 1 + \lvert J/2C \rvert$
$2C = \sqrt{\Delta\nu^2 + J^2}$	$\nu_3 = \nu_{av.} + \frac{1}{2}S_i$	Total intensity $I_T = 4$
$S_i = 2C - J$	$\nu_4 = \nu_{av.} + \frac{1}{2}S_o$	
$S_o = 2C + J$		

Scheme 4.

Very often a direct analysis of a many-line $[AR_tX_n]_2$ system proves to be impossible, so simulations including lineshape calculations are desirable. For effective computation, we chose to rewrite the algebraic expressions given above. When the parameter ranges $0 \cdots \chi$ or $\lambda \cdots t$ and $0 \cdots \mu$ or $\nu \cdots n$ are introduced, expressions for the $(t + 1)^2(n + 1)^2$ ab-type subspectra are obtained [equations (x)—(xii)]. The total intensity for an A spectrum is $I_T = 2^{2(t + n + 1)}$.

$$\nu_{av.} = \nu_A + \tfrac{1}{2}[(\chi + \lambda)N_{AR} + (\mu + \nu)N_{AX}] \quad \text{(x)}$$

$$\Delta\nu = (\chi - \lambda)L_{AR} + (\mu - \nu)L_{AX} \quad \text{(xi)}$$

$$I = 4\binom{t}{\chi}\binom{t}{\lambda}\binom{n}{\mu}\binom{n}{\nu} \quad \text{(xii)}$$

Our program DOK178,[14,*] designed on the basis given above, permits successive simulations of A spectra in $[AR_tX_n]_2$ systems as a function of L_{AR}, L_{AX}, $J_{AA'}$, and a common spectral linewidth (using a Lorentzian shape). In the studies presented here, ^{31}P n.m.r. spectra of $[CH_3(t\text{-}C_4H_9)P(X)]_2Y$ follow the pattern described above.

Deceptively Simple A *Spectra from* $[AR_tX_n]_2$ *Systems.*—If $|J_{AA'}|$ is much larger than both $|L_{AR}|$ and $|L_{AX}|$, or, more accurately, if $|J_{AA'}| \gg |(\chi - \lambda)L_{AR} + (\mu - \nu)L_{AX}|$ for all subspectra of significant statistical weight, a deceptively simple $(2t + 1)(2n + 1)$ line pattern will result, as would be the case for an $AR_{2t}X_{2n}$ system. The residual transition frequencies are given by equation (xiii) and the intensities by (xiv). No information on $J_{AA'}$, L_{AR}, or L_{AX} may be obtained from such spectra, which will yield only ν_A, N_{AR}, and N_{AX}. An example of this situation is found in $[CH_3(t\text{-}C_4H_9)P]_2$, (1b).

$$\Delta\nu = \nu_A + \tfrac{1}{2}[(\chi + \lambda)N_{AR} + (\mu + \nu)N_{AX}] \quad \text{(xiii)}$$

$$I = 4\binom{2t}{\chi + \lambda}\binom{2n}{\mu + \nu} \quad \text{(xiv)}$$

In cases of vanishing $J_{AA'}$ the A spectrum may be described as simple overlapping first-order multiplets having $(t + 1)^2$-$(n + 1)^2$ lines with repeated spacings J_{AR}, $J_{AR'}$, J_{AX}, and $J_{AX'}$.

* Copies are available from the authors.

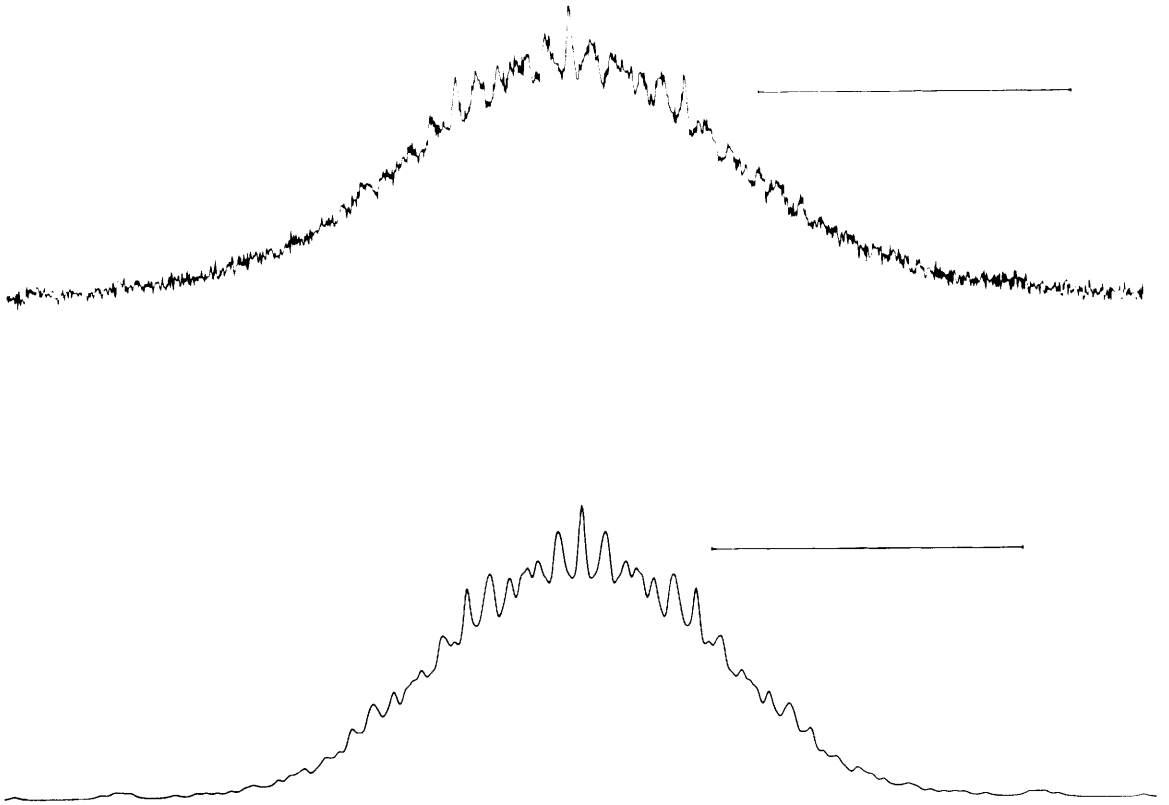

Figure 1. Experimental (upper) and simulated (lower) ^{31}P n.m.r. spectrum of *meso*-$[CH_3(t\text{-}C_4H_9)P(S)]_2O$ (3a). Calibration bar 50 Hz

Table 1. Explicit expressions for the frequencies and intensities of R and X χ lines in $[AR_tX_n]_2$ n.m.r. spectra

ν	Frequency	Intensity
ν_{1R}	$\nu_R + \frac{1}{2}(T_1 + T_{2R})$	$\frac{1}{2}(1 - g_R)T_{3R}T_{4R}T_{5X}$
ν_{2R}	$\nu_R + \frac{1}{2}(T_1 - T_{2R})$	$\frac{1}{2}(1 + g_R)T_{3R}T_{4R}T_{5X}$
ν_{3R}	$\nu_R - \frac{1}{2}(T_1 - T_{2R})$	$\frac{1}{2}(1 + g_R)T_{3R}T_{4R}T_{5X}$
ν_{4R}	$\nu_R - \frac{1}{2}(T_1 + T_{2R})$	$\frac{1}{2}(1 - g_R)T_{3R}T_{4R}T_{5X}$
ν_{1X}	$\nu_X + \frac{1}{2}(T_1 + T_{2X})$	$\frac{1}{2}(1 - g_X)T_{3X}T_{4X}T_{5R}$
ν_{2X}	$\nu_X + \frac{1}{2}(T_1 - T_{2X})$	$\frac{1}{2}(1 + g_X)T_{3X}T_{4X}T_{5R}$
ν_{3X}	$\nu_X - \frac{1}{2}(T_1 - T_{2X})$	$\frac{1}{2}(1 + g_X)T_{3X}T_{4X}T_{5R}$
ν_{4X}	$\nu_X - \frac{1}{2}(T_1 + T_{2X})$	$\frac{1}{2}(1 - g_X)T_{3X}T_{4X}T_{5R}$

The Spectra of the R_t *and* X_n *Groups.*—The appearance of R_t and X_n spectra is again governed by symmetry. These spectra are symmetrically placed about ν_R and ν_X respectively. Half of each total intensity is due to pairs of strong lines separated by N_{AR} and N_{AX}, respectively. These pairs will be called N lines. The remaining half of each intensity is contributed by so-called χ lines. $2t(n + 1)$ χ_R sets and $2n(t + 1)$ χ_X sets exist, each responsible for two pairs of centrosymmetric lines which will be named *inner* and *outer* χ lines. The following parameters (or ranges) are used: $-t \cdots \chi_R \cdots +t$; $-n \cdots \chi_X \cdots +n$; $\alpha_R = |\chi_R - \frac{1}{2}| - \frac{1}{2}$; $\alpha_X = |\chi_X - \frac{1}{2}| - \frac{1}{2}$; $\Sigma_1 = \chi_R L_{AR} + \chi_X L_{AX}$; $\Sigma_{2R} = (\chi_R - 1)L_{AR} + \chi_X L_{AX}$; $\Sigma_{2X} = (\chi_X - 1)L_{AX} + \chi_R L_{AR}$; $T_1 = [\Sigma_1^2 + J_{AA'}^2]^{\frac{1}{2}}$; $T_{2R} = [\Sigma_{2R}^2 + J_{AA'}^2]^{\frac{1}{2}}$; $T_{2X} = [\Sigma_{2X}^2 + J_{AA'}^2]^{\frac{1}{2}}$; $T_{3R} = \frac{1}{2}(t - \alpha_R)$; $T_{3X} = \frac{1}{2}(n - \alpha_X)$; $T_{4R} = \binom{2t}{t - \alpha_R}$; $T_{4X} = \binom{2n}{n - \alpha_X}$; $T_{5R} = \binom{2t}{n - |\alpha_R|}$; $T_{5X} = \binom{2n}{n - |\alpha_X|}$; $g_R = (\Sigma_1\Sigma_{2R} + J_{AA'}^2)/T_1T_{2R}$; and $g_{11} = (\Sigma_1\Sigma_{2X} + J_{AA'}^2)/T_1T_{2X}$.

Explicit equations for transition frequencies and intensities of the χ_R and χ_X line sets are listed in Table 1. The N_{AR} and χ_R lines add up to $t\,2^{(2t + n + 1)}$ in intensity, and N_{AX} and χ_X lines to $n\,2^{(2t + n + 1)}$. The equations given in Table 1 are modifications of our previous results,[4-6] suitable for efficient programming. Our program DOK177 [14] allows for successive simulations of R_t and X_n group spectra in $[AR_tX_n]_2$ systems. Specific values for the widths of N_{AR}, χ_{AR}, N_{AX}, and χ_{AX} lines may be separately assigned to simulate the total n.m.r. spectrum using Lorentzian lineshapes.

Proton n.m.r. spectra of $[CH_3(t\text{-}C_4H_9)P(X)]_2Y$ obey the rules given in the above section.

Deceptively simple R_t *and* X_n *Group Spectra.*—If $J_{AA'}^2$ is very large compared to Σ_1^2, Σ_{2R}^2, and Σ_{2X}^2 for all values of χ_R and χ_X with significant statistical probability (close to $\frac{t}{2}$ and $\frac{n}{2}$) the R_t and X_n spectra exhibit the typical features of *deceptively simple triplets*. This situation holds for ^1H n.m.r. spectra of $[CH_3(t\text{-}C_4H_9)P]_2$, (1b). The only information then obtained directly comprises the Larmor frequencies, N_{AR}, and N_{AX}. No information about L_{AR}, L_{AX}, and $J_{AA'}$ is accessible.

In cases of vanishing $J_{AA'}$ particularly primitive spectra result. Each group (R_t and X_n) will give rise to doublets of doublets separated by J_{AR},$J_{AR'}$ and J_{AX},$J_{AX'}$ respectively.

Spectral Analysis and Simulation of $[AR_tX_n]_2$ *Systems for* $[CH_3(t\text{-}C_4H_9)P(X)]_2Y$ *Compounds.*—The previous section listed explicit expressions for transition frequencies and intensities of A nuclei and R_t and X_n groups for $[AR_tX_n]_2$ systems. Here we demonstrate typical spectral features of those systems, using $[CH_3(t\text{-}C_4H_9)P(X)]_2Y$ as examples. The experimental and simulated n.m.r. spectra are shown in Figures 1—3 (^{31}P) and 4—6 (^1H).

Numerical results from our observations on compounds having directly bonded P–P structures, $[CH_3(t\text{-}C_4H_9)P(X)]_2$

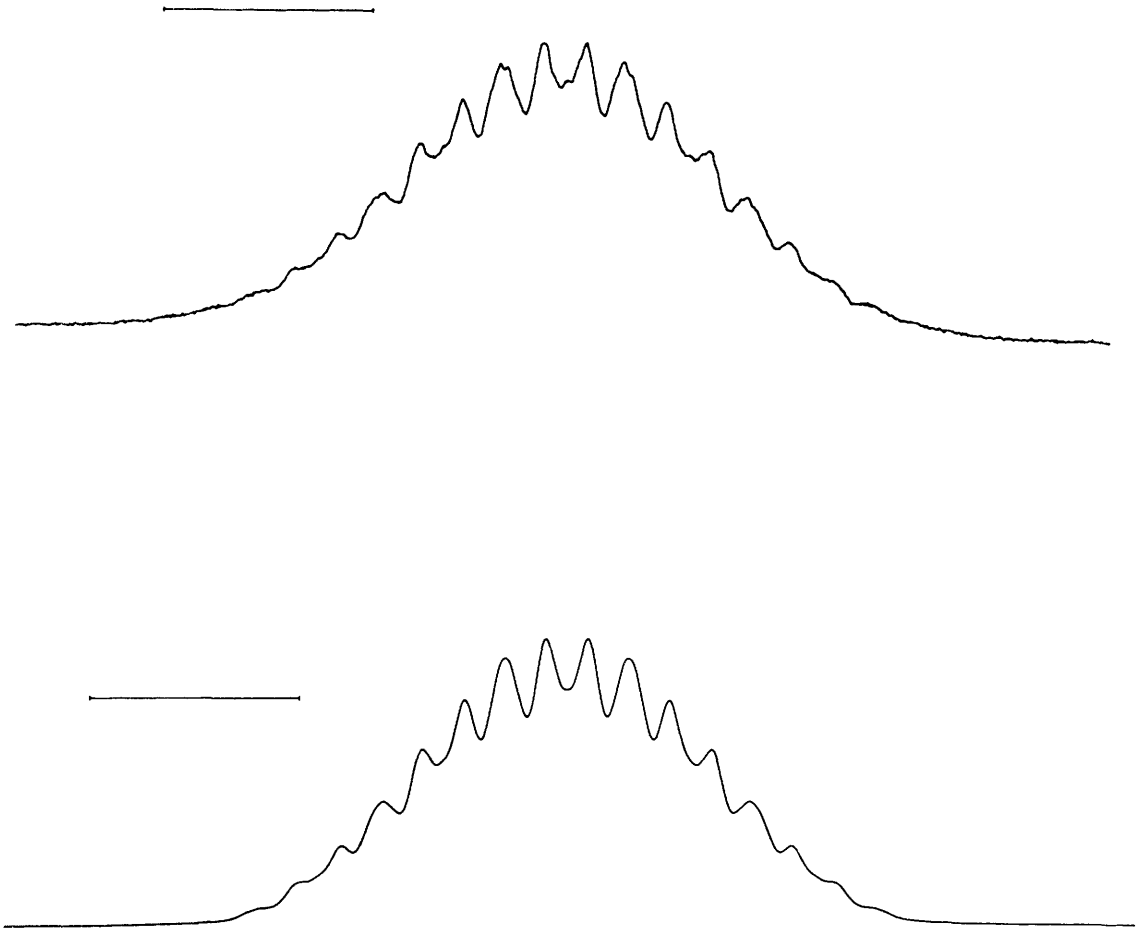

Figure 2. ^{31}P N.m.r. spectrum of *rac*-$[CH_3(t\text{-}C_4H_9)P(S)]_2$ (2b) as in Figure 1. Calibration bar 30 Hz

Table 2. $[AR_rX_n]_2$ N.m.r. parameters (in Hz) for diphosphanes $[CH_3(t\text{-}C_4H_9)P]_2$ and $[CH_3(t\text{-}C_4H_9)P(S)]_2$

Compound	(1b)	(2a)	(2b)
Form	*rac*	*meso*	*rac*
N_{AR}	8.0	5.23	4.55 ± 0.5
L_{AR}	3.0	17.93	19.0 ± 0.5
N_{AX}	12.65	13.35	18.1 ± 0.5
L_{AX}	11.8	16.85	18.1 ± 0.5
$J_{AA'}$	293 ± 1	97 ± 1	120 ± 1
h.w. (A)	1.6	—	3.0
h.w. (N_{AR})	0.35	0.8	0.5
h.w. (χ_R)	0.4	1.2	1.15
h.w. (N_{AX})	0.5	0.8	0.5
h.w. (χ_X)	0.9	1.2	0.95

h.w. = linewidth at half-height (from comparison of experimental and simulated spectra).

Table 3. Proton and phosphorus-31 n.m.r. data [a] for $[CH_3(t\text{-}C_4H_9)P]_2$ and $[CH_3(t\text{-}C_4H_9)P(S)]_2$

Compound	(1b)	(2a)	(2b)
Form	*rac*	*meso*	*rac*
$J_{AR} = {}^2J_{PH}$	±5.5	−11.58	−11.78
$J_{AR'} = {}^3J_{PPCH}$	+2.5	+6.35	+7.23
$J_{AX} = {}^3J_{PPCH}$	+12.2	+17.10	+18.10
$J_{AX'} = {}^4J_{PPCCH}$	+0.4	+0.25	$-0.25 < J_{AX'} < 0.25$
$J_{AA'} = {}^1J_{PP}$	(−)293 ± 1	(−)97 ± 1	(−)120 ± 1
$\delta_A = \delta_P$	−30.67 −31.73	54.00	59.392
$\delta_H(R_r) = \delta_H(PCH_3)$	0.915 [b]	1.684	1.662
$\delta_H(X_n) = \delta_H(CCH_3)$	1.114	1.235	1.317
Solvent	Dioxane [b] or C_6D_6 [c]	$C_6D_5CD_3$	C_6D_6
Concentration (%)	25	25	25

[a] The coupling constants are given in Hz and the chemical shifts in p.p.m. [b] ^{31}P spectra for dioxane solution. [c] ^1H spectra for C_6D_6 solution.

(X = lone pair or S), (1b), (2a), and (2b), are given in Tables 2 and 3. Corresponding data for bridged P–Y–P systems, $[CH_3(t\text{-}C_4H_9)P(S)]_2Y$ (Y = O or S), (3a), (3b), (4a), and (4b), follow in Tables 4 and 5. In addition, results for unsymmetrical molecules $CH_3(t\text{-}C_4H_9)P(S)\text{–}Y\text{–}P(t\text{-}C_4H_9)CH_3$ (Y = — or S), (5a), (5b), (6a), and (6b), are given in Tables 6 and 7. These compounds involve spin systems of $ABR_3S_3X_9Y_9$ type (Scheme 5). The corresponding spectra are first order, and analysis in principle should be trivial since in each case $|\nu_A - \nu_B| \gg |J_{AB}|$. Data for such compounds were obtained from an equilibrated mixture following the general equation (xv). Details of this redistribution reaction will be given elsewhere.[1] Nine individual proton resonance bands for CH_3 and $t\text{-}C_4H_9$ groups in each of the compounds (1b), (5a), (5b), (6a), and (6b) were assigned

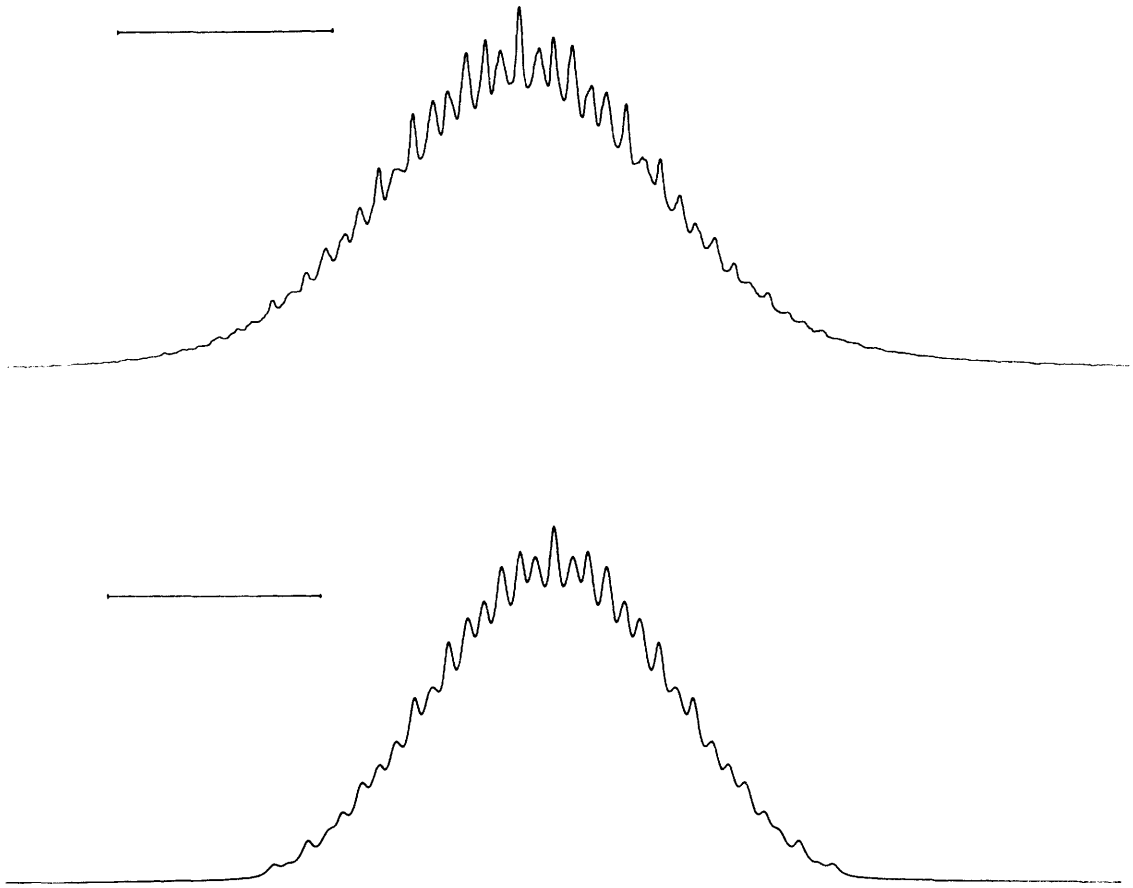

Figure 3. ^{31}P N.m.r. spectrum of *rac*-$[CH_3(t\text{-}C_4H_9)P]_2$ (1b) as in Figure 1. Calibration bar 25 Hz

Table 4. $[AR_nX_n]_2$ N.m.r. parameters (in Hz) for $[CH_3(t\text{-}C_4H_9)P(S)]_2Y$

Compound	(3a)	(4b)
Y	O	S
Form	*meso*	*rac*
N_{AR}	11.70	11.9 ± 0.1
L_{AR}	12.20	14.0 ± 0.25
N_{AX}	18.40	18.9 ± 0.1
L_{AX}	18.40	18.9 ± 0.25
$J_{AA'}$	56	17.0 ± 0.5
h.w. (A)	1.7	—
h.w. (N_{AR})	0.5	0.5
h.w. (χ_R)	0.75	1.0
h.w. (N_{AX})	0.5	0.8
h.w. (χ_X)	0.8	1.5

Table 5. Proton and ^{31}P n.m.r. data * for $[CH_3(t\text{-}C_4H_9)P(S)]_2Y$

Compound	(3a)	(3b)	(4a)	(4b)
Y	O	O	S	S
Form	*meso*	*rac*	*meso*	*rac*
$J_{AR} \equiv {}^2J_{PCH}$	−11.95	—	—	+13.0
$J_{AR'} \equiv {}^4J_{PYPCH}$	+0.25	—	—	+1.0
$J_{AX} \equiv {}^3J_{PCCH}$	+18.4	—	—	+18.9
$J_{AX'} \equiv {}^5J_{PYPCCH}$	0	—	—	0
$J_{AA'} \equiv {}^2J_{PYP}$	(−)56 ± 1	—	—	(−)17 ± 1
$\delta_A \equiv \delta_P$	110.81	109.746	91.026	90.825
$\delta_H(R_t) \equiv \delta_H(PCH_3)$	1.76	—	1.900	2.217
$\delta_H(X_n) \equiv \delta_H(CCH_3)$	1.19	—	1.136	1.049
Solvent	C_6D_6	$C_6D_5CD_3$	$C_6D_5CD_3$	$C_6D_5CD_3$
Concentration (%)	25	3	5	5

* Coupling constants are given in Hz and chemical shifts in p.p.m.

specifically using lineshape simulations for 90-, 360-, and 500-MHz ^1H n.m.r. spectra.

$$[CH_3(t\text{-}C_4H_9)P]_2 + [CH_3(t\text{-}C_4H_9)P(S)]_2 \rightleftharpoons$$
(1b) (2b)

$$2\ CH_3(t\text{-}C_4H_9)P(S)\text{-}Y\text{-}P(t\text{-}C_4H_9)CH_3 \quad (xv)$$
(5a), (5b), (6a), (6b)

Discussion

Crystal-structure determinations by *X*-ray techniques for diphosphanes are sparse,[15,16] and, in any case, not necessarily relevant to the solution state. They suggest that a conformation approaching the semi-eclipsed is favoured in some cases, but an *anti* conformation in others. The stability of conformations near the semi-eclipsed is supported by empirical force-field calculations,[17] although applications of *ab-initio* SCF-MO theory to P_2H_4 itself show [18] a relatively flat potential minimum extending from the *gauche* to the *trans* conformation, with the former only slightly favoured (optimum dihedral angle 76°).

Crystal-structure work by Lee and Goodacre [19,20] has established that the *trans* conformation is favoured for two cyclic diphosphane disulphides and the parent $[(CH_3)_2P(S)]_2$.[21]

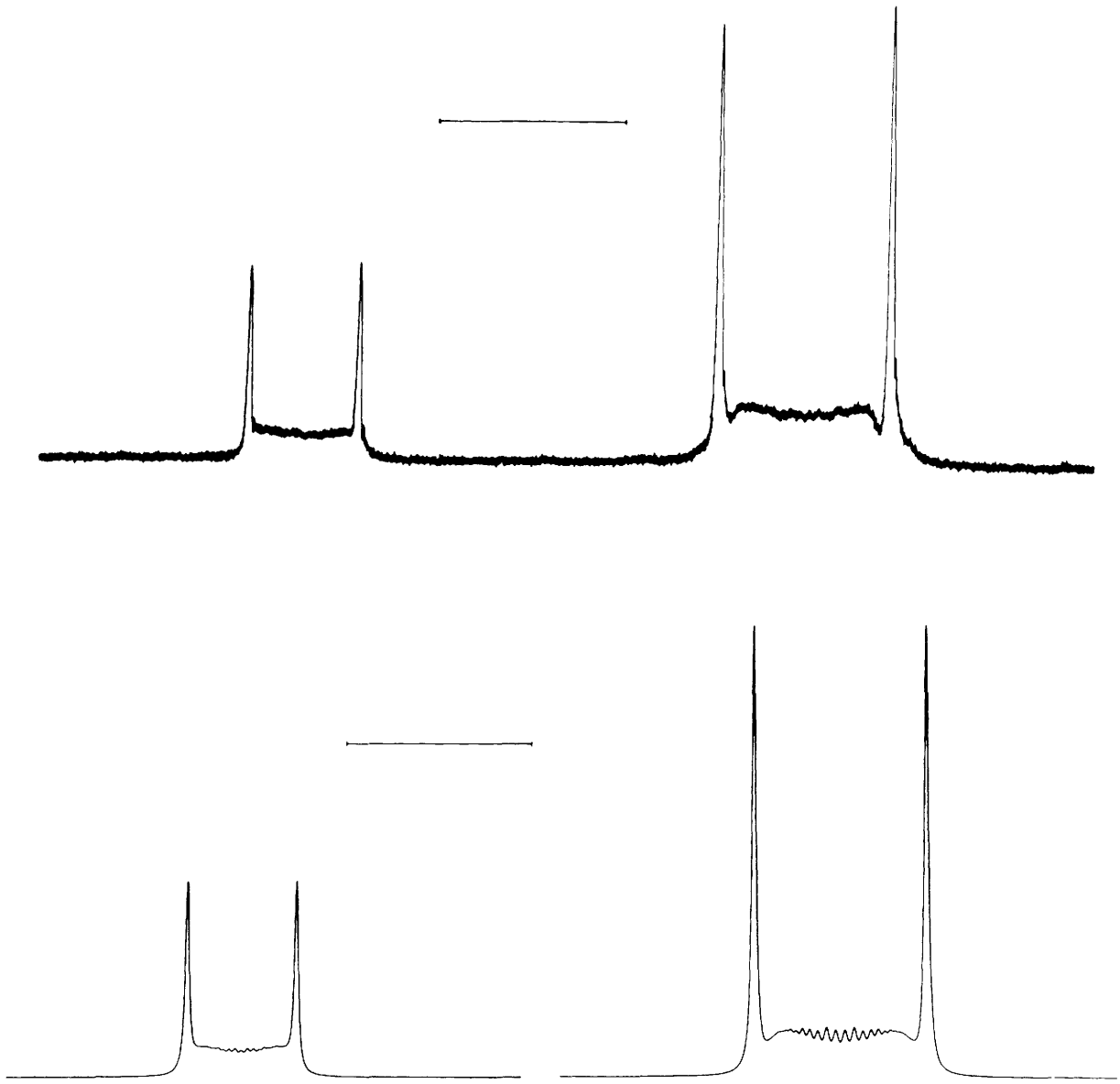

Figure 4. Experimental (upper) and simulated (lower) ^1H n.m.r. spectrum of *meso*-$[CH_3(t\text{-}C_4H_9)P(S)]_2O$ (3a). Calibration bar 20 Hz. Left, CH_3 group; right, $t\text{-}C_4H_9$ group

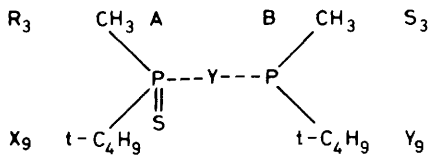

Scheme 5.

Wunderlich and Wussow [2] deduced unequivocally the existence of the all-*trans* conformation for our model system, *meso*-diphosphane disulphide (2a). The same authors presented [2] the first example known of a gauchoid diphosphane disulphide, compound (2b). The molecular structures of (2a) and (2b) in the solid state are shown in Figures 7 and 8. P–O–P and P–S–P bridged structures for *meso* (3a) and *rac* (4b) were determined by Mootz and co-workers.[3] Results for corresponding *X*-ray studies may be seen in Figures 9 and 10; for details see Parts 2 and 3 of this series.[2,3] As far as we know, there are no reported *X*-ray crystallographic studies of compounds of the types (5) and (6).

Some n.m.r. data have been presented previously [4,6,7,10,22] for compounds (1) and (2), and, where relevant, our results are in reasonable agreement with the earlier work. McFarlane and McFarlane [7] established that the sign of $^1J_{PP}$ is negative for both these compounds. The variation of $^1J_{PP}$ for diphosphanes with dihedral angle has been the subject of a number of theoretical investigations,[22-27] and it seems to be generally agreed that the most negative value of $^1J_{PP}$ would be given by the conformation with eclipsed lone pairs. However, it is very likely that other factors, such as substituent bulk, are also of great importance in governing the value of $^1J_{PP}$. Moreover, Tutunjian and Waugh [28] have shown that the anisotropy in J_{PP} is much larger than the isotropic average for $[(C_2H_5)_2P(S)]_2$, thus rendering problematic discussion of solution-state results from J_{PP}.

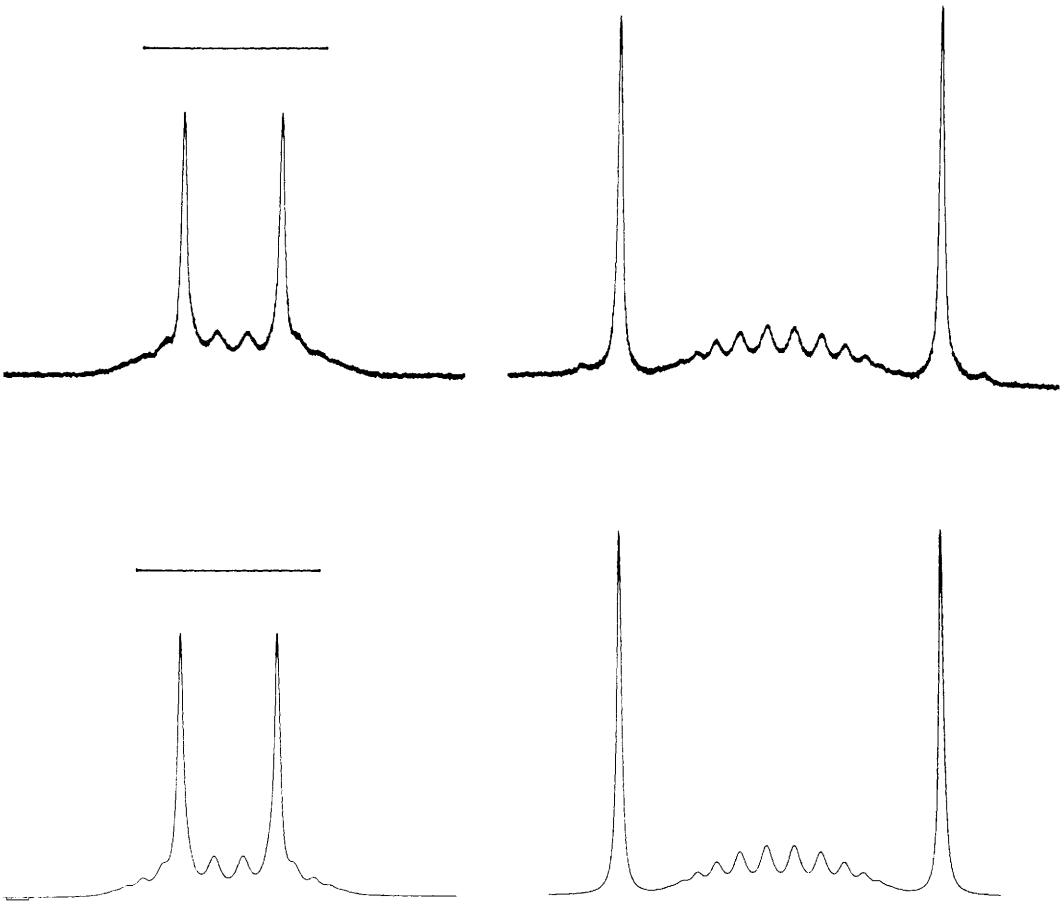

Figure 5. Proton n.m.r. spectrum of *meso*-$[CH_3(t\text{-}C_4H_9)P(S)]_2$ (2a) as in Figure 4. Calibration bar 10 Hz

Table 6. N.m.r. data [a] for $CH_3(t\text{-}C_4H_9)P(S)\text{–}P(t\text{-}C_4H_9)CH_3$ and $CH_3(t\text{-}C_4H_9)P(S)\text{–}S\text{–}P(t\text{-}C_4H_9)CH_3$

Compound	(5a)	(5b)		(6a)	(6b)
Form	*meso*	*rac*		*meso*	*rac*
$J_{AR} \equiv {}^2J_{PCH}$	−11.20	−11.28	$^2J_{PCH}$	−11.54	−11.54
$J_{AS} \equiv {}^3J_{PPCH}$	+2.57	0	$^4J_{PSPCH}$	0	0.86
$J_{AY} \equiv {}^3J_{PCCH}$	+12.44	13.04	$^3J_{PCCH}$	+16.93	+18.21
$J_{AX} \equiv {}^4J_{PPCCH}$	0.81	0.81	$^5J_{PSPCCH}$	+6.67	+7.69
$J_{BS} \equiv {}^2J_{PCH}$	−15.05	−17.78	$^2J_{PCH}$	−18.29	−14.96
$J_{BR} \equiv {}^3J_{PPCH}$	6.24	0	$^4J_{PSPCH}$	0	0
$J_{BX} \equiv {}^3J_{PCCH}$	+16.16	16.25	$^3J_{PCCH}$	+12.65	+12.74
$J_{BY} \equiv {}^4J_{PPCCH}$	0	0	$^5J_{PSPCCH}$	0	0
$J_{AB} \equiv {}^1J_{PP}$	(−)294.2	312.5	$^2J_{PSP}$	54.8	51.3
$\delta_A \equiv \delta_P(P^V)$	59.99	54.55	$\delta_P(P^V)$	87.83	85.80
$\delta(R_t) \equiv \delta_H(PCH_3)$	1.5658	1.3679	$\delta_H(PCH_3)$	1.7896	1.7154
$\delta(X_n) \equiv \delta_H(CCH_3)$	1.0520	1.3173	$\delta_H(CCH_3)$	1.2588	1.1846
$\delta_B \equiv \delta_P(P^{III})$	−28.73	−28.80	$\delta_P(P^{III})$	40.76	41.02
$\delta(S_t) \equiv \delta_H(PCH_3)$	0.9338	0.8986	$\delta_H(PCH_3)$	1.1769	1.0678
$\delta(Y_n) \equiv \delta_H(CCH_3)$	1.0776	1.1424	$\delta_H(CCH_3)$	1.044	1.0165
Solvent	C_6D_6	C_6D_6		C_6D_6	C_6D_6
Concentration [b] (%)	7	4		3	1.5

[a] The coupling constants are given in Hz and the chemical shifts in p.p.m. For the designations A, B, R, S, X, and Y see Scheme 5. [b] Mixture of products, see text.

The data presented here confirm that inclusion of bulky t-butyl substituents substantially increases the magnitude of J_{PP} in both series (1) and (2). Moreover, $|J_{PP}|$ appears to be larger for the *rac* form than for the *meso* form in compounds (2a), (2b) and (5a), (5b), although the situation is not clear for series (1).[10,29-32] Differences in J_{PP} between *rac* and *meso* forms are presumably related to changes in rotamer populations and/or in the dihedral angles for the most stable rotamers. This should be true for series (2) and (5) as well as (1). Since the alkyl substituents in the compounds studied here are markedly

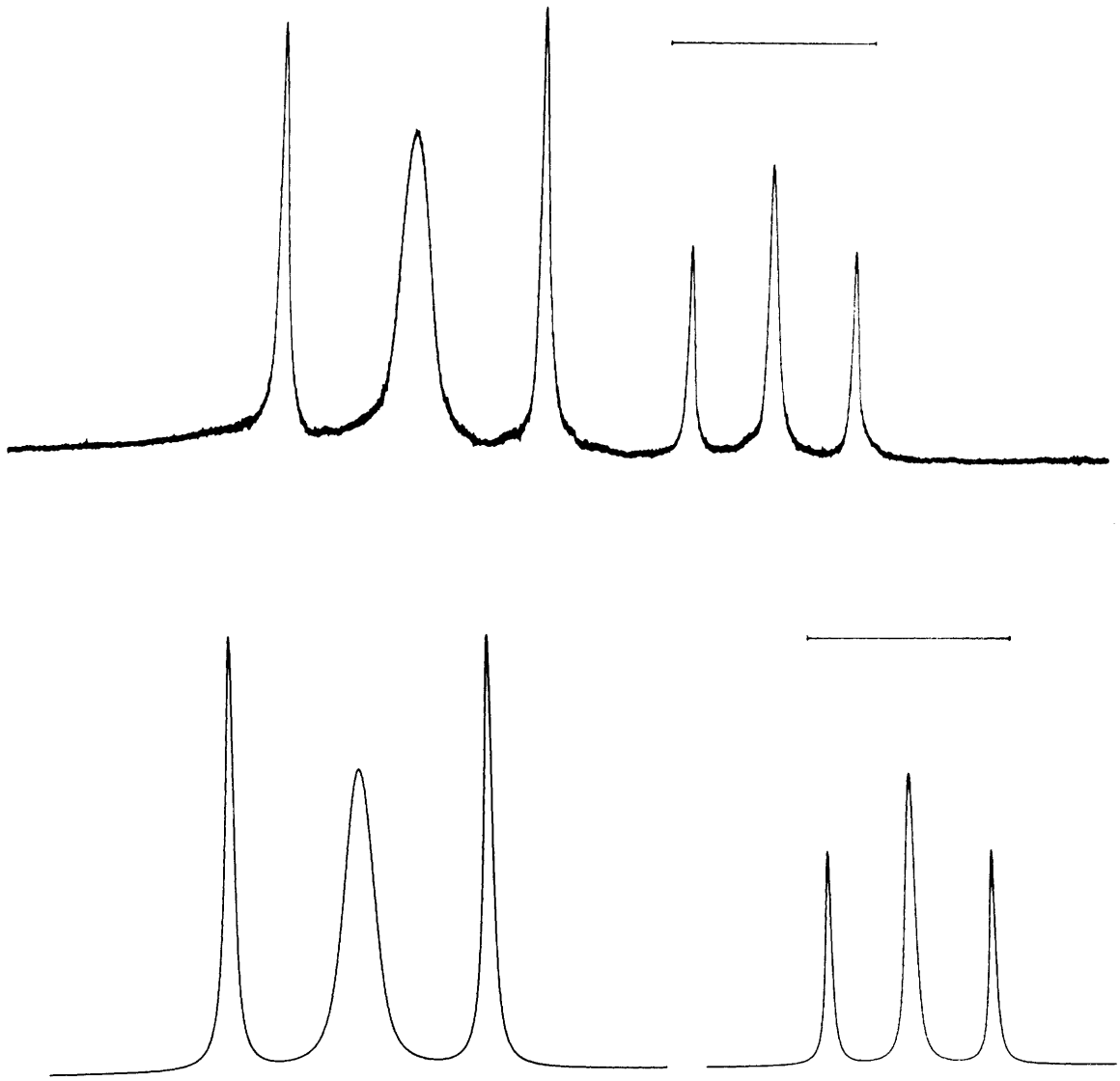

Figure 6. Proton n.m.r. spectrum of *rac*-$[CH_3(t\text{-}C_4H_9)P]_2$ (1b) as in Figure 4. Calibration bar 10 Hz

different in bulk (CH_3 and $t\text{-}C_4H_9$), variations in n.m.r. parameters between the two diastereoisomers might be expected to be substantial. This scarcely seems to be the case for J_{PP} in (5a), (5b), and although our value for the difference in J_{PP} between (2a) and (2b) is large in terms of percentage, this is not true for the results reported by McFarlane and McFarlane.[7]

The inclusion of sulphur as a substituent presumably imparts additional rigidity to molecular structures.[7] This is perhaps reflected in the fact that J_{PP} values for compounds (1) and (5) are similar, whereas those for (2) are much smaller, which is true for the tetramethyl compounds as well as for those studied here.

The two-bond (P,P) coupling constants found for compounds (3a), (4b) and (6a), (6b) are smaller than the values of $^1J_{PP}$ discussed above, and this is in line with results for related compounds.[33] Few conclusive comments can be made on the (P,H) coupling constants, especially as there is an inherent ambiguity between the long- and short-range data. In general, the changes induced in these parameters by the replacement of CH_3 by $t\text{-}C_4H_9$ are not large except in the case of $[(CH_3)_2P]_2$

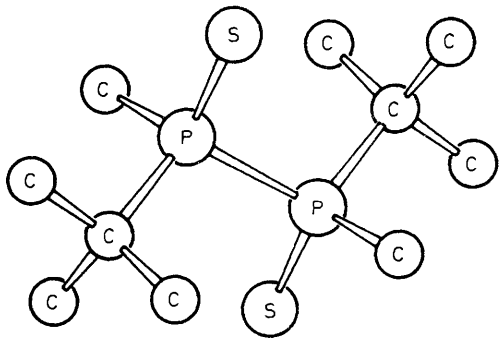

Figure 7. Molecular structure of *meso*-$[CH_3(t\text{-}C_4H_9)P(S)]_2$ (2a)

and $[CH_3(t\text{-}C_4H_9)P]_2$. The phosphorus chemical shifts follow the patterns established for the corresponding tetramethyl compounds, although there is a pronounced deshielding effect of replacing CH_3 by $t\text{-}C_4H_9$. Such deshielding has been dis-

Table 7. Hypothetical *N*-type and *L*-type values (in Hz) for $CH_3(t\text{-}C_4H_9)P(S)\text{–}Y\text{–}P(t\text{-}C_4H_9)CH_3$*

Compound	(5a)	(5b)	(6a)	(6b)
Y	—	—	S	S
Form	*meso*	*rac*	*meso*	*rac*
$N_{ARS} = J_{AR} + J_{AS}$	8.63	11.28	11.54	10.68
$L_{ARS} = J_{AR} - J_{AS}$	13.77	11.28	11.54	12.40
$N_{AXY} = J_{AX} + J_{AY}$	13.25	13.85	23.60	25.90
$L_{AXY} = J_{AX} - J_{AY}$	11.63	12.23	10.26	10.52
$N_{BSR} = J_{BS} + J_{BR}$	8.79	17.78	18.29	14.96
$L_{BSR} = J_{BS} - J_{BR}$	21.29	17.78	18.29	14.96
$N_{BYX} = J_{BY} + J_{BX}$	16.16	16.25	12.25	12.74
$L_{BYX} = J_{BY} - J_{BX}$	16.16	16.25	12.25	12.74
J_{AB}	(−)294.2	(−)312.5	54.8	51.3

* For the spin-system notation, see Scheme 5. Absolute values of the coupling parameters are given.

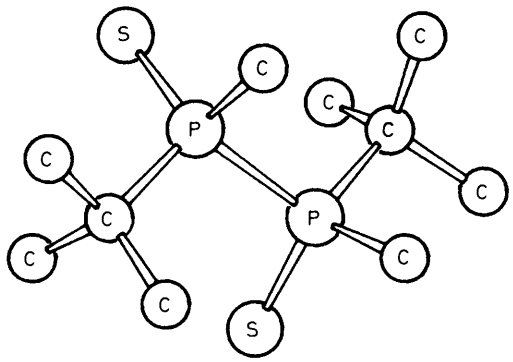

Figure 8. Molecular structure of *rac*-$[CH_3(t\text{-}C_4H_9)P(S)]_2$ (2b)

cussed [10,29,34] for compounds related to (1) in terms of β- and γ-substituent effects.

Experimental

For synthetic routes to compounds (1)—(6) see refs. 1, 3, and 7. The samples were dissolved in the relevant solvent, $SiMe_4$ added, and the solutions filtered into 5-mm and 10-mm n.m.r. tubes as appropriate. The tubes were then sealed after application of the conventional freeze–pump–thaw technique. 90-MHz Proton n.m.r. spectra were obtained using a Bruker HX90R spectrometer at Düsseldorf. For the continuous-wave mode the following conditions were applied: chart scale 1 Hz cm^{-1}, scan speed 0.06 Hz s^{-1}, with an accuracy in frequency measurement of ±0.1 Hz. Phosphorus-31 n.m.r. spectra were run in the Fourier-transform mode at 36.43 MHz. Data for compounds (5) and (6) were extracted from 360-MHz and 500-MHz ^1H n.m.r. spectra obtained from Dr. D. Wendisch, Bayer AG, and Dr. W. Hull, Bruker Analytische Meßtechnik GmbH. Chemical shift data (δ_H) in Tables 3, 5, and 6 are referenced to internal $SiMe_4$. For ^{31}P shifts the data in these Tables are presented with respect to external H_3PO_4 [setting δ_P (85% H_3PO_4) = 0 from an independent measurement on 85% H_3PO_4]. Lineshape simulations were performed using computer programs DOKI77 and DOKI78, arranged for the Telefunken TR 445 computer at Düsseldorf. Satisfying lineshapes in $[AR_tX_n]_2$ systems resulted when specific linewidths were used for *N* and χ lines separately. Different accuracies for data reported in Tables 2—7 resulted from the use of 90-MHz, 360-MHz, and 500-MHz spectrometers, from

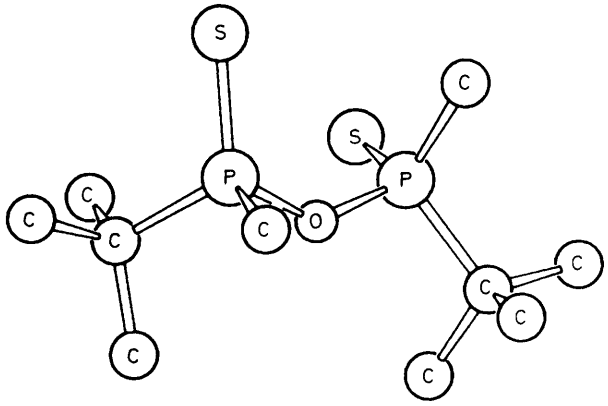

Figure 9. Molecular structure of *meso*-$[CH_3(t\text{-}C_4H_9)P(S)]_2O$ (3a)

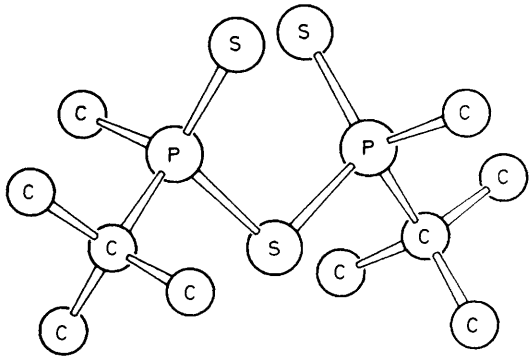

Figure 10. Molecular structure of *rac*-$[CH_3(t\text{-}C_4H_9)P(S)]_2S$ (4b)

direct readings of δ_H and *N* values respectively, and from lineshape simulations leading to *L* and $J_{AA'}$ data.

Acknowledgements

We thank the N.A.T.O. Scientific Affairs Division for a grant enabling the co-operation to take place between the German and British groups. In addition, support from the Fonds der Chemischen Industrie and a research grant from Nordrhein-Westfalen is acknowledged. Thanks are due to Drs. Wendisch and Hull for help with 360-MHz and 500-MHz n.m.r. spectra.

References

1 Part 1, G. Hägele, G. Tossing, and J. Seega, *Z. Naturforsch.*, in the press.
2 Part 2, H. Wunderlich and H. G. Wussow, *Z. Naturforsch.*, in the press.
3 Part 3, G. Hägele, W. Kückelhaus, D. Mootz, and H. Wunderlich, *Phosphorus Sulfur*, in the press.
4 G. Hägele, Habilitationsschrift, Universität Düsseldorf, 1972.
5 G. Hägele and R. K. Harris, *Ber. Bunsenges. Phys. Chem.*, 1972, **76**, 910.
6 G. Hägele, R. K. Harris, and J. Nichols, *J. Chem. Soc., Dalton Trans.*, 1973, 79.
7 H. C. E. McFarlane and W. McFarlane, *J. Chem. Soc., Chem. Commun.*, 1975, 582.
8 H. C. E. McFarlane and W. McFarlane, *Chem. Commun.*, 1971, 1589.
9 R. K. Harris, E. M. McVicker, and M. Fild, *J. Chem. Soc., Chem. Commun.*, 1975, 886.
10 S. Aime, R. K. Harris, E. M. McVicker, and M. Fild, *J. Chem. Soc., Dalton Trans.*, 1976, 2144.

11 J. B. Lambert, G. F. Jackson, and D. C. Mueller, *J. Am. Chem. Soc.*, 1968, **90**, 6401; 1970, **92**, 3093.
12 A. A. Bothner-By and C. Naar-Colin, *J. Am. Chem. Soc.*, 1962, **84**, 743.
13 R. K. Harris, *Can. J. Chem.*, 1968, **42**, 2275.
14 DOKI77, DOKI78 G. Hägele and W. Kückelhaus, 1977—1978.
15 R. Richter, J. Kaiser, J. Sieler, H. Hartung, and C. Peter, *Acta Crystallogr., Sect. B*, 1977, **33**, 1887.
16 S. G. Baxter, A. H. Cowley, R. E. Davis, and P. E. Riley, *J. Am. Chem. Soc.*, 1981, **103**, 1699.
17 S. G. Baxter, D. A. Dougherty, J. P. Hummel, J. F. Blount, and K. Mislow, *J. Am. Chem. Soc.*, 1978, **100**, 7795.
18 A. H. Cowley, D. J. Mitchel, M. H. Whango, and S. Wolfe, *J. Am. Chem. Soc.*, 1979, **101**, 5224.
19 J. D. Lee and G. W. Goodacre, *Acta Crystallogr., Sect. B*, 1969, **25**, 2127.
20 J. D. Lee and G. W. Goodacre, *Acta Crystallogr., Sect. B*, 1970, **26**, 507.
21 J. D. Lee and G. W. Goodacre, *Acta Crystallogr., Sect. B*, 1970, **27**, 303.
22 H. C. E. McFarlane and W. McFarlane, *J. Chem. Soc., Dalton Trans.*, 1980, 240.
23 A. H. Cowley, W. D. White, and M. C. Damaso, *J. Am. Chem. Soc.*, 1974, **91**, 1922.
24 R. K. Safiullin, Y. Y. Samitov, and R. M. Minova, *Teor. Eksp. Khim.*, 1974, **10**, 828.
25 J. P. Albrand, H. Faucher, G. Gagnaire, and J. B. Robert, *Chem. Phys. Lett.*, 1976, **38**, 521.
26 A. A. M. Ali, Ph.D. Thesis, University of East Anglia, 1979.
27 V. Galasso, *J. Magn. Reson.*, 1979, **36**, 181.
28 P. N. Tutunjian and J. S. Waugh, *J. Chem. Phys.*, 1982, **76**, 1223.
29 A. A. M. Ali and R. K. Harris, *J. Chem. Soc., Dalton Trans.*, 1983, 583.
30 J. P. Albrand and G. Gagnaire, *J. Am. Chem. Soc.*, 1972, **94**, 8630.
31 J. P. Albrand and J. B. Robert, *J. Chem. Soc., Chem. Commun.*, 1976, 876.
32 J. P. Albrand and C. Taieb, *J. Am. Chem. Soc. Symp. Ser.*, 1981, **171**, 577.
33 G. Hägele, W. Kuchen, and W. Steinberger, *Z. Naturforsch., Teil B*, 1979, **29**, 349.
34 A. A. M. Ali, G. Bocelli, R. K. Harris, and M. Fild, *J. Chem. Soc., Dalton Trans.*, 1980, 638.

Received 1*st March* 1984; *Paper* 4/348